Spin echo of nuclei in domain walls of yttrium orthoferrite crystals

A. V. Zalesskiĭ, A. K. Zvezdin, V. G. Krivchenko, A. M. Balbashov, T. A. Khimich, and E. A. Evdishchenko

Crystallography Institute, USSR Academy of Sciences

An experimental study was made of the spin-echo spectra of ^{57}Fe nuclei in the domain walls of YFeO$_3$ crystals grown by various methods. It is shown that echo signals are observed from nuclei located on the "edge" of the wall. In the presence of an external permanent magnetic field the echo signals continue to be formed in a certain layer next to the domain. This leads to substantial differences in the character of the evolution of the spectra previously investigated by a stationary NMR procedure. This layer extends to different depths in crystals grown by different methods. The formation of the echo signal in domain walls of a YFeO$_3$ crystal are considered with allowance for the specific features of its magnetic properties, and the theoretical spectra are compared with the experimental ones. The peculiarities of the spectra can be satisfactorily explained theoretically only when account is taken of the variation of the time of the transverse relaxation over the wall thickness and of the change of the NMR frequencies inside the wall, which is characteristic of orthoferrites.

PACS numbers: 75.60.Ch, 76.60.Lz, 76.60.Es

INTRODUCTION

NMR of ^{57}Fe nuclei in the domain walls of orthoferrites, particularly in the case of the YFeO$_3$ crystal, is characterized by a number of remarkable peculiarities, which consist in the following. The NMR spectrum obtained for YFeO$_3$ by a stationary procedure in a zero external field consists of two closely lying resonant . lines at the frequencies ω_{max} and ω_{min}.[1,2] The existence of these lines is due to the presence of two frequency branches inside the domain walls.[3] When account is taken of the external permanent magnetic field H_x, directed along the a axis of a rhombic crystal, the angular dependence of the intraboundary frequency branches for crystals having the magnetic symmetry typical of orthoferrites is written in the form[1-3]

$$\omega(\varphi) = \omega_d(1 - \alpha \sin^2\varphi \mp \beta \sin 2\varphi) \pm \gamma_n H_x \cos\varphi, \qquad (1)$$

where α and β are certain phenomenological constants of the hyperfine interaction and are determined from experiment, ω_d is the NMR frequency in the domain ($\varphi = 0$ and 180°), γ_n is the nuclear gyromagnetic ratio (it is equal to 0.138 MHz/kOe for ^{57}Fe nuclei), and φ is the angle of rotation of the ferromagnetism vector in the (ac) plane relative to the c axis (or of the antiferromagnetism vector relative to the a axis). The presence in YFeO$_3$ of 180° walls with rotation of the spin in the (ac) plane follows from NMR data.[1] The frequencies ω_{max} and ω_{min} (or ν_{max} and ν_{min} if the frequencies are expressed in MHz) correspond to a maximum spectral spin density satisfying the condition $d\omega(\varphi)/d\varphi = 0$. It is typical that resonance signals at the frequencies ω_{max} and ω_{min} are due to nuclei located in different sections of the wall: the higher-frequency line corresponds to nuclei located closer to the domain, while the second line corresponds to nuclei closer to the center of the wall.

If the crystal is exactly oriented relative to the external constant magnetic field, the domain walls of TFeO$_3$ can be preserved without a noticeable change in their internal structure in relatively strong fields (10 kOe and more) perpendicular to the "easy" axis c. This makes it possible to study the properties of the intraboundary NMR in the presence of the field H_x [the field H_y along the b axis exerts no influence on the NMR spectra, since the hyperfine fields in the walls are located in the plane $(xz) = (ac)$].

The influence of the field H_x on the stationary NMR spectra is quite unique. With increasing H_x, the frequencies ω_{max} and ω_{min} come asymmetrically closer together until they merge completely in a certain critical field, which is approximately 5 kOe for the hydrothermal crystal YFeO$_3$ at 77 K. With further increase of H_x, the reonance is washed out. In the course of the evolution of the spectrum in the field H_x the coordinates of the nuclei responsible for their resonance lines vary in a complicated manner inside the wall, with a tendency to shift towards the center of the wall. For the sake of clarity, one can refer to Fig. 4 below, where the arrows show the displacements of the frequencies ν_{max} and ν_{min} (Fig. 4 will be discussed in detail in § 4).

It is enticing to use this unique property of the NMR spectra to "probe" the wall over its thickness. For example, it is of interest to use the spin-echo method to study the distribution of the relaxation times inside the wall. The first information on the observation of an intraboundary spin echo in YFeO$_3$ in a zero external field was reported in Ref. 4. The echo signals were observed only in the region of the high-frequency line. We have undertaken a detailed investigation of the spin-echo spectra in a field H_x, on the same hydrothermal crystals previously investigated by the continuous procedure. The results recently published in Ref. 5 have shown that the character of the spin-echo spectra and its evolution in the field H_x differ substantially from the "stationary" case. The echo signals were excited by the domain walls, but were observed at frequencies that are more typical of the domains.

0038-5646/81/061300-07$02.40

The tasks undertaken in this study were the following. First, a detailed study of the features of the nuclear spin echo and of the domain walls of the $YFeO_3$ crystals, both in the absence of an external field and at $H_x \neq 0$. Second, an attempt was made to explain the observed spectrum with the aid of existing theoretical notions concerning the mechanism which the nuclear echo is produced in domain walls. Third, to analyze the causes of the differences between the results obtained by the continuous procedure and by the spin-echo method. Of additional interest was the use of NMR on $YFeO_3$ crystals grown not only under hydrothermal conditions but also by other methods.

§1. SAMPLES AND EXPERIMENTAL PROCEDURE

We used yttrium-orthoferrite crystals grown by two methods: hydrothermal at our Institute (hereafter referred to as crystal 1), and by zone melting, without a crucible, using radiation heating,[6] at the Problems Laboratory of the Moscow Engineering Institute (crystal 2). Crystal 1 was included among these previously used to study NMR by the continuous procedure. Attempts, by any of the procedures, to observe intra-boundary NMR signals in $YFeO_3$ crystals grown from solution in the melt or by the Verneuil method were unsuccessful, apparently because of the lower mobilities of the domain walls in these crystals.

The hydrothermal crystal, measuring approximately $1 \times 1 \times 0.5$ cm, had a characteristic faceting with which it could be easily oriented relative to the crystallographic axes. Crystal 2 was approximately of the same volume, but was initially cylindrical in shape, and was oriented by the x-ray method. After orientation, it was cut along a plane perpendicular to the c axis, after which the a and b axes were marked on this plane.

The NMR investigation by the continuous procedure, just as in the earlier studies,[1,2] was carried out with the aid of a supergenerator. To observe the spin echo, we used an ISSh-1-13 pulsed spectrometer designed by the special design office of the Institute of Radio and Electronics of the USSR Academy of Sciences. This spectrometer can record automatically the amplitude of the echo signal as a function of the varying pulse carrier frequency. The spectrometer is not designed to work with the low-power pulses necessary to observe the interboundary NMR characterized by high values of the gain η. To weaken the intensity of the radio-frequency (RF) field H, the spectrometer modulator was connected to an external supply source with decreased voltage. In addition, the coil of the high-frequency push-pull generator, consisting of two sections, was wound in a manner such as to cancel out almost completely the resultant intensity H_1.

The best regime for obtaining an echo signal in both crystals was a sequence of two short pulses of almost equal duration, $\tau = 1.5$–2 μsec, with a pulse-pair repetition frequency 100–200 Hz. The pulses were followed by a rather prolonged (15–20 μsec) induction signal, and therefore the time interval τ_{12} between the pulses was usually chosen to be close to 40 μsec. The constant field was produced by the electromagnet of

the EPR spectrometer with sufficient high field homogeneity.

The transverse-relaxation time T_2 was determined by the standard method, by measuring the decrease of the echo amplitude with increasing τ_{12}. The longitudinal relaxation time T_1 was measured by the three-pulse procedure. All the results are reported for a temperature 77 K.

§2. EXPERIMENTAL RESULTS

To verify that the main regularities of the stationary NMR spectra, previously observed in hydrothermal crystals, remain in force also for a crystal obtained by zone melting, we have measured, using a supergenerator, the NMR spectra in the field H_x at 77 K for the crystal 2. Just as for the crystal 1, the spectrum consists of two resonance lines, which come closer together with increasing H_x. The points in Fig. 1 show the measured line frequencies in the field H_x, while the solid curves 2 show the theoretical shift of the frequencies ν_{max} and ν_{min}, determined from Eq. (1) under the condition $d\omega(\varphi)/d\varphi = 0$. The reduction of the results consisted mainly of finding the best fit of the theoretical curves plotted for different ratios α/β to the experimental points (the plotting of these curves is described in greater detail in Ref. 2). The best agreement for crystal 2 is reached at the values of α, β, and ν_d indicated in Table I. Figure 1 shows for comparison (curve 1) the frequency shift for crystal 1 in accord with the data of Ref. 1 (the experimental points have been left out). The values α, β, and ν_d for crystal 1 are also given in Table I.

A comparison shows that the crystals grown by different methods differ principally in the values of the parameter α, which determines the NMR frequency $\nu_d(1 - \alpha)$ at the center of the domain wall. Since the properties at the center of the wall are most strongly influenced by processes connected with thermal vibrations of the wall (Winter magnons), it follows that in crystals that differ in the character of the impurities and in the degree of perfection (because of different growth conditions) one can expect the largest difference precisely in the value of α. The decrease, by a factor of 2, of the parameter α for crystal 2 has caused the frequency ν_{min} for this crystal to be approximately 0.05 MHz higher than for the crystal 1, and the merging of the frequency branches takes place in somewhat weaker fields.
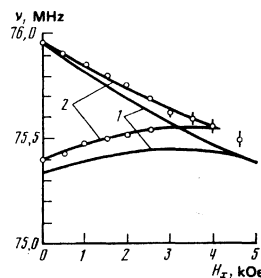

FIG. 1. Shift of NMR frequencies in field H_x for crystal 1 (curves 1) and crystal 2 (curves 2), according to the data obtained by the stationary procedure.

TABLE I.

	Crystal 1	Crystal 2		Crystal 1	Crystal 2
α	$5.6 \cdot 10^{-3}$	$3.2 \cdot 10^{-3}$	η_0	$2 \cdot 10^6$	$2 \cdot 10^6$
β	$2.8 \cdot 10^{-3}$	$3.2 \cdot 10^{-3}$	a	$3.6 \cdot 10^{-3}$	$3.6 \cdot 10^{-3}$
ν_d	75.85 MHz	75.81 MHz	τ_{12}	40 μsec	40 μsec
τ	1.5 μsec	1.5 μsec	T_{20}	3.2 μsec	16 μsec
Q	360	360	c	25	5
H_i	10^{-3} Oe	10^{-3} Oe			

In all other respects, the character of the evolution of the static NMR spectra for crystals 1 and 2 is the same.

Figure 2 shows examples of the spin-echo spectra for these same two crystals. Let us stop to discuss the most characteristic singularities of these crystals.

Crystal 1. This spectrum at $H_x = 0$ consists of one asymmetrical peak with a gentle decline towards lower frequencies, and with a maximum that almost coincides with the frequency ν_{max} of the high-frequency line of the stationary spectrum. We were unable to obtain an echo signal, in the region of the low-frequency line (75.35 MHz), although a distinct maximum of the induction signal is observed at this frequency. With increasing H_x, the spectrum first became narrower ($H_x < 0.6$ kOe), and then split into two lines that moved apart almost linearly from H_x, with slopes close to $\pm\gamma_n H_x$. The shift of the maxima in the field H_x for crystal 1 is shown by the dark circles in Fig. 3.

Crystal 2. At $H_x = 0$, two maxima are observed in the spectrum. One of them (high-frequency) is close as before to ν_{max}, and the second, although close to the

FIG. 3. Shift of the maxima in the spin-echo spectra in the field H_x for crystal 1 (dark circles) and for crystal 2 (light circles). The solid lines correspond to the frequencies for $\varphi = 9°$ (crystal 1) and $\varphi = 18°$ (crystal 2).

stationary line at the frequency $\nu_{max} = 75.4$ MHz (Fig. 1), lies approximately 0.08 MHz above the latter. With increasing H_x, the lines come closer together, they are superimposed in the interval $1 < H_x < 1.5$ kOe (at this instant the spectrum is narrowest, most symmetrical, and most intense), and then at $H_x > 1.5$ kOe the spectrum splits, just as for crystal 1. The main peak continues to shift towards lower frequencies, while a weaker maximum splits away from it on the high-frequency side and shifts towards the high frequencies (Fig. 2). The shifts of the maxima in the field H_x for crystal 2 are shown in Fig. 3 by light circles.

Table II shows the values of the relaxation times T_1 and T_2 for crystals 1 and 2. The values of T_1 and T_2 differ little for the two crystals. A characteristic feature is the fact that the relaxation time corresponding to the diverging branches on Fig. 3 are the same and remain unchanged with increasing H_x.

Thus, comparing the results obtained by the stationary method and by the spin-echo method, we see that they differ substantially from each other. The stationary method always consists of two lines that come closer together with increasing H_x and become washed out after they merge. In the spin-echo spectrum, a low-frequency signal may not appear (crystal 1), and instead of the gradual approach of the lines, two diverging branches, with no noticeable tendency to become washed out or to vanish, are observed past a certain value of H_x. In the next sections we shall attempt to ascertain the causes of this difference.
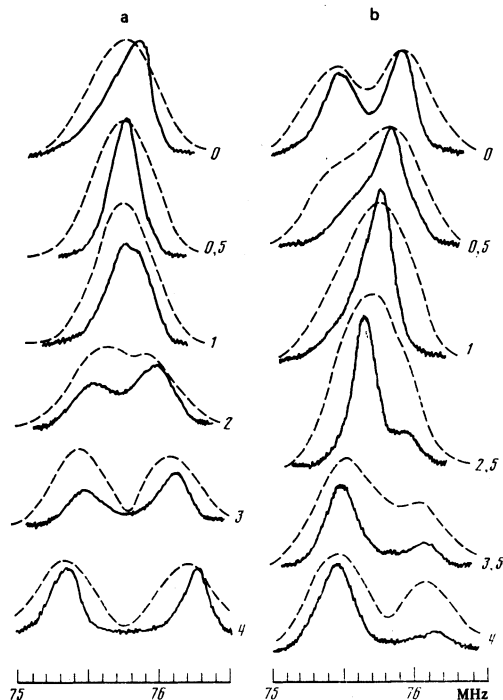

FIG. 2. Experimental and theoretical (dashed lines) spin-echo spectra: a—for crystal 1, b—for crystal 2. The numbers indicate the values of H_x in kOe. The amplitudes of the theoretical spectra are normalized in such a way that the height of the peak at $H_x = 0$ (which is the largest for the crystal 2) coincides with the experimental one.
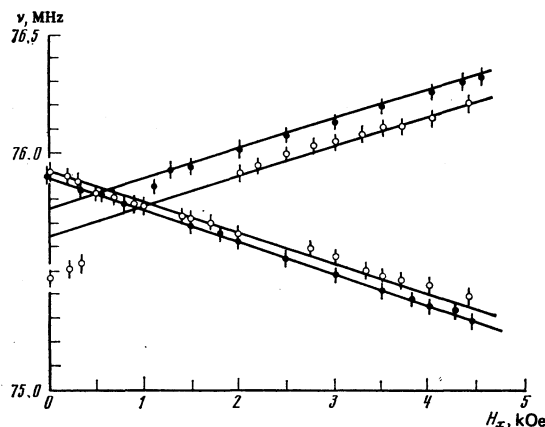
TABLE II.

H_x, kOe	Crystal 1		Crystal 2	
	T_1, μsec	T_2, μsec	T_1, μsec	T_2, μsec
0	400–500	120–180	700–900 * 300–500 **	150–170 * 70–100 **
1–4 ***	200–400	70–90	–	80–120

*For the high-frequency peak; **for the low-frequency peak; ***values of T_1 and T_2 are the same for both diverging branches.

§3. THEORY AND COMPARISON WITH EXPERIMENT

The sequence of the physical processes that take place in the spin echo of nuclei located in domain walls is the following. The external RF field causes a periodic displacement of the domain walls, and by the same token leads to oscillations of the hyperfine field at the nuclei. As a result of the action of two RF pulses, an echo signal is produced in the nuclear system. The precession of the nuclear spins during the time of appearance of the echo induces, via the hyperfine interaction, vibrations of the domain walls, and consequently causes a change in the magnetization of the sample, which is in fact registered by the receiving coil.

Assume that the demagnetized crystal contains a strip domain structure of the open type with period $2W$, and that the plane of the walls coincides with the (ac) plane of the crystal, in which the spin rotation takes place. The motion of the domain wall under the influence of the RF field, with account taken of the hyperfine interaction, will be described by an equation similar to that proposed in Refs. 7 and 8:

$$m\ddot{q} + \frac{2M_s}{\mu}\dot{q} + m\omega_r^2 q = 2M_s H_1(t) - \delta U, \qquad (2)$$

where q is the shift of the center of the domain wall, M_s is the saturation magnetization (the ferromagnetism vector in the case of YFeO$_3$), m and μ are the effective mass and mobility of the domain wall; for the weak ferromagnet YFeO$_3$ they are given by[9] $m = 2M_s/\gamma^2 H_D$ and $\mu = M_s/\Gamma m\gamma H_E$, where $\gamma = 1.76 \times 10^7$ rad/sec, $H_D = 1.4 \times 10^5$ Oe is the Dzyaloshinskiĭ field, $H_E = 6.4 \times 10^6$ Oe is the exchange field acting between the sublattices. $\delta = (A/K_1)^{1/2}$ is the domain-wall thickness, A is the exchange rigidity, K_1 is the corresponding anisotropy constant, and $\Gamma \approx 10^{-5}$ ($T = 300$ K) is the Gilbert damping con-constant. The quantity ω_r in (2) is the resonance frequency of the domain wall (in a perfect crystal it is determined by the magnetostatic interaction); $H_1(t)$ is the external RF field and is directed along the $c(z)$ axis; $-\delta U$ is the pressure exerted on the domain wall by the precessing nuclear spins via the hyperfine interaction. This pressure is equal to

$$\delta U = \frac{C\omega_d}{\gamma_n} \int_{-\infty}^{+\infty} \mu_{nx}^{loc}(\varphi)\left(\frac{d\varphi}{dy}\right) dy. \qquad (3)$$

In (3), $C \approx 0.02$ is the concentration of the ^{57}Fe isotope, and φ and γ_n were defined above. In the calculation of δU followed by that of the gain η, the hyperfine field is taken to be ω_d/γ_n, since the anisotropic part of $\omega(\varphi)$ in (1), which is less than 1% of ω_d, can be neglected in the present case. The integration in (3) is with respect to the coordinate y, which varies along the normal to the wall. The quantity μ_{nx} is the projection of the nuclear magnetization, corresponding to the coordinate y, on the x axis of the local coordinate system, chosen such that its z axis coincides with the direction of the antiferromagnetism vector at the point with coordinate y, the x axis lies in the (ac) plane, and the y axis coincides with the b axis of the crystal. The z axis of the local system lags the a axis of the crystal by an angle φ.

Expression (3) can be given the following physical

meaning. The quantity $-C\omega_d\mu_{nx}^{loc}/\gamma_n$ is the torque produced by the hyperfine interaction and acting on the magnetic moments of the ions, whose direction is determined by the angle φ. Multiplying it by $d\varphi$ and integrating, we obtain the total moment acting on the domain wall and due to the nuclei. The first term in the right-hand side of (2) can be also interpreted in the same way: the quantity $-M_s H_1 \sin\varphi$ is the moment applied to the spins by the external field. By multiplying by $d\varphi$ and integrating from 0 to π, we obtain a pressure $2M_s H_1(t)$ on the wall.

The magnetic moments of the nuclei have also a component μ_{ny}^{loc}, but it does not produce a torque, by virtue of the almost scalar nature of the hyperfine interaction (the small anisotropy of the hyperfine interaction can here also be neglected), and because the y component of the magnetic moments of the ions is zero with a high degree of accuracy.

The projection of the RF field on the x axis of the local coordinate frame is equal to

$$H_x^{eff} = H_1 \sin\varphi + \frac{\omega_d}{\gamma_n}\frac{d\varphi}{dy} q(t) \approx \eta_0 H_1(t)\sin\varphi. \qquad (4)$$

The gain η_0 corresponding to the center of the domain wall is a complex quantity. Hereafter we shall take η_0 to mean its modulus, equal to

$$|\eta_0| = \frac{2M_s\omega_d\mu}{\delta\gamma_n[m^2\mu^2(\omega_p^2-\omega^2)^2 - 4M_s^2\omega^2]^{1/2}}, \qquad (5)$$

where ω is the frequency of the RF field H_1 that causes the vibrations of the wall. We note that the gain for the "inverse" process, of the action of the nuclear system and the domain wall, due to the term δU in (2), is equal to $C\eta_0$.

The dependence of μ_{nx}^{loc} on the angle φ and on the time is determined by the Bloch equations. To determine $\mu_{nx}^{loc}(\varphi, t)$ we can use the results of Refs. 10 and 11, in which a matrix method was developed for calculating the dynamics of the nuclear magnetization when it is acted upon by different sequences of pulses. In our case, according to Refs. 10 and 11, μ_{nx}^{loc} can be represented in the form

$$\mu_{nx}^{loc}(t) = \mu_1 \cos(\omega t + \psi) - \mu_2 \sin(\omega t + \psi), \qquad (6)$$

where μ_1 and μ_2 are the x' and y' components of the nuclear magnetization in a coordinate frame rotating with velocity ω. The time t is reckoned from the instant of termination of the second RF pulse, and ψ is the phase of the rotating coordinate system at $t = 0$, and is of no importance in what follows. The values of μ_1 and μ_2 for two pulses of equal duration τ with an interval τ_{12} are determined by the formulas

$$\mu_1 = -2\mu_{n0}\,\mathrm{Re}[\,(\beta_1^*)^2\beta_1\alpha_1\exp[2i\Delta\omega(t-\tau_{12})]\,]\exp\left(-\frac{t+\tau_{12}}{T_2(\varphi)}\right), \qquad (7)$$

$$\mu_2 = -2\mu_{n0}\,\mathrm{Im}[\,(\beta_1^*)^2\beta_1\alpha_1\exp[2i\Delta\omega(t-\tau_{12})]\,]\exp\left(-\frac{t+\tau_{12}}{T_2(\varphi)}\right), \qquad (8)$$

$$\alpha_1 = \cos\frac{b\tau}{2} - i\cos\theta\sin\frac{b\tau}{2}, \quad \beta_1 = -i\sin\theta\sin\frac{b\tau}{2},$$

$$\mathrm{tg}\,\theta = \frac{\gamma_n\eta_0 H_1\sin\varphi}{\Delta\omega}, \quad \Delta\omega = -\omega + \omega(\varphi),$$

$$b = [(\Delta\omega)^2 + (\gamma_n\eta_0 H_1)^2\sin^2\varphi]^{1/2},$$

where μ_{n0} is the equilibrium magnetization of the nu-

clear system, $T_2(\varphi)$ is the transverse relaxation time, which for nuclei inside the wall is a function of the angle φ, and $\omega(\varphi)$ and η_0 are defined by formulas (1) and (5), respectively.

Substituting (6), (7), and (8) in Eq. (2) and integrating the latter, we obtain the quantity $q(t)$, which determines the ac component of the crystal magnetization

$$M(t) = \frac{2M_s}{W} q(t). \qquad (9)$$

The emf E induced in the receiving coil can be expressed as follows

$$E = kSdM/dt, \qquad (10)$$

where S is the area of the sample surface normal to the easy magnetization axis, and k is the dimensionless coefficient of the coupling between the receiving coil and the magnetic system.

Thus, formulas (6)–(10) together with (2) determine completely the time dependence of the echo signal. In the immediate proximity to the instant $t = \tau_{12}$, the calculation procedure can be simplified. In this case, according to (6), (7), and (8), μ_{nx}^{loc}, and consequently $q(t)$ and $E(t)$, are harmonic functions of the time. For the signal amplitude we obtain after simple calculations the formula

$$|E| \propto \left| \frac{J_1 - i 2 J_2}{\omega_p^2 - \omega^2 - i\omega (2M_s/\mu m)} \right| = E_0 [J_1^2 + 4J_2^2]^{1/2}, \qquad (11)$$

$$E_0 = \frac{2kSM_sC\omega_d\omega\mu_{n0}}{W\gamma_n m[(\omega_p^2 - \omega^2)^2 + \omega^2(2M_s/\mu m)^2]^{1/2}},$$

$$J_1 = \int_0^\pi d\varphi \sin^3\theta \sin^2\frac{b\tau}{2} \sin b\tau \exp\left(-\frac{2\tau}{T_2(\varphi)}\right),$$

$$J_2 = \int_0^\pi d\varphi \sin^3\theta \sin^4\frac{b\tau}{2} \cos\theta \exp\left(-\frac{2\tau}{T_2(\varphi)}\right).$$

A formula similar to (11), but with a different coefficient E_0, was used in Ref. 12.

For the calculation, it is more convenient to transform (11) into

$$E(\Omega) = \text{const} \cdot (I_1^2 + Q^2 I_2^2)^{1/2}, \qquad (12)$$

$$I_1 = \int_0^\pi \psi(\varphi) \sin^3\varphi \exp(-c\sin^2\varphi) d\varphi, \qquad (13)$$

$$I_2 = \int_0^\pi u(\varphi) \sin^3\varphi [\Omega(\varphi) - \Omega] \exp(-c\sin^2\varphi) d\varphi. \qquad (14)$$

In (12)–(14) are introduced the following symbols:

$$Q = \frac{\omega_d\tau}{2}, \quad \psi(\varphi) = \frac{\sin^2\Delta}{\Delta^2}\frac{\sin 2\Delta}{2\Delta}, \quad u(\varphi) = \frac{\sin^4\Delta}{\Delta^4},$$

$$\Delta = \frac{b\tau}{2} = Q[(1 - \Omega - \alpha\sin^2\varphi - \beta\sin 2\varphi + h\cos\varphi)^2 + a^2\sin^2\varphi]^{1/2}.$$

For convenience in the calculation we used in (12)–(14) the normalized dimensionless quantities:

$$\Omega(\varphi) = \frac{\omega(\varphi)}{\omega_d}, \quad \Omega = \frac{\omega}{\omega_d}, \quad h = \frac{\gamma_n H_x}{\omega_d}, \quad a = \frac{\gamma_n H_1\eta_0}{\omega_d}.$$

The angular dependence of the relaxation time $T_2(\varphi)$ was taken in the form

$$T_2 = T_{20}/\sin^2\varphi,$$

where T_{20} is the minimum transverse-relaxation time

in the center of the wall. The parameter c in (13) and (14) is connected in the following manner with T_{20} and the time interval τ_{12} between the pulses:

$$c = 2\tau_{12}/T_{20}.$$

Thus, the amplitude of the echo becomes a function of the following parameters:

$$E(\Omega, \alpha, \beta, Q, a, h, c) \propto (I_1^2 + Q^2 I_2^2)^{1/2}.$$

The form of the spectrum $E(\Omega)$ was calculated with a computer. The values of the different parameters that fit the experiment best are given in Table I. We used for the calculation the same values of α, β, and ω_d as for the stationary spectra. The quantities τ and τ_{12} were taken to correspond to the real experimental conditions. The least accurate estimates are those of H_1 and η_0, the product of which gives a transverse high-frequency component of the local field at the nuclei. The value $\eta_0 = 2 \times 10^6$ indicated in Table I was taken from the experimental data for $YFeO_3$ at 77 K, given in Ref. 4. The best agreement with experiment is reached at $a = 3.6 \times 10^{-3}$, which corresponds to a value of H_1 on the order of 10^{-3} Oe. The value of the shortest time of transverse relaxation T_{20}, which enters in the parameter c, is not known from experiment. However, as will be shown in §4, the values of T_{20} given in Table I do correspond to the real situation.

The computer-calculated spectra are shown by dashed lines in Fig. 2. Although no complete agreement between the form of the spectra is observed (the calculated spectra are broader), the theoretical spectra reflect correctly the most characteristic features of the experimental spectra and their evolution in the field H_x.

§4. DISCUSSION OF RESULTS

The main result that follows from the analysis of the theoretical spectra is that when no account is taken of the time of transverse relaxation over the wall thickness [of the parameter c in (13) and (14)], agreement with experiment is impossible at any value of any other parameter in (12). In particular, it is impossible to obtain agreement for the characteristic "parting" of the high-frequency branch in the spectra at $H_x > 1$ kOe (Fig. 2 and 3). It can therefore be assumed that the influence of the relaxation processes in formation of nuclear echo in the walls is one of the main causes of the difference between the results obtained by the pulse method and by the continuous procedure, when the relaxation processes can be disregarded.

Computer calculation of the spectra by formula (12) does not show where the nuclei that make the main contribution to the echo signals are localized in the wall. We shall attempt to analyze this question separately.

Figure 4 shows the NMR frequency branches inside the wall (half of the wall is shown) at different values of H_x, plotted for crystal 2 in accord with the parameters α, β, and ν_d indicated in Table I. To gain a clear idea of the distribution of the frequencies over the thickness of the wall, the horizontal scale was chosen to be linear in the dimensionless coordinate $\xi = \pi y/\delta$. The connection of ξ with the angle φ is given by the known

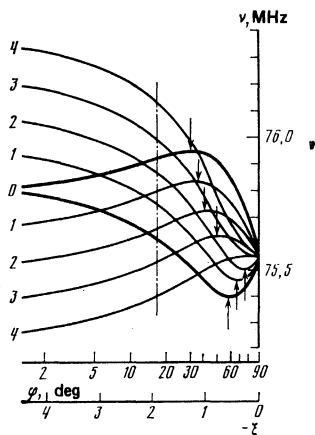1304   Sov. Phys. JETP 53(6), June 1981

Zalesskiĭ et al.   1304

FIG. 4. Dependence of NMR frequencies inside the domain wall (half of the wall is shown), for crystal 2, on the coordinate ξ and on the angle φ at different values of H_x. The values of H_x (in kOe) are indicated to the left of the curves. The arrows show how the frequencies corresponding to curves 2 of Fig. 1 are shifted. The section $\varphi = 18°$ is shown by the dashdot line.

Landau-Lifshitz formula: $\cos\varphi = -\tanh\xi$. In this scale, the nuclei in the interior of the domain $(\xi = 0)$ are located at $\xi \to -\infty$, the center of the wall corresponds to $\xi = 0$ $(\varphi = 90°)$, and the "classical" width of the wall δ is equal to π (the theoretical thickness of the wall for YFeO$_3$ is of the order of 500–1000 A).

It follows from Fig. 4 that in the central part of the wall there are no nuclei with frequencies corresponding to the diverging branches of Fig. 3. The presence of these branches can be explained if it is assumed that the echo signals are formed by nuclei located in a certain layer inside the wall, corresponding to relatively small angles φ. For crystal 2, good agreement with experiment is obtained if it is assumed that this layer corresponds to angles near $\varphi = 18°$ (or 162°). The solid lines drawn in Fig. 3 through the light circles (for crystal 2) refer to frequencies corresponding to the intersection of the curves of Fig. 4 by the dashed line at $\varphi = 18°$. The obtained functions $\nu(H_x)$ hardly differ from linear. Except for the points relating to the high-frequency maximum in fields $H_x < 0.5$ kOe, the experimental values of the frequencies fit the calculated lines satisfactorily.

It is possible to obtain in similar fashion the frequency corresponding to the experimental data for crystal 1. We recall that for crystal 1 the value of the parameter α is approximately double that of crystal 2, therefore the $\nu(\varphi)$ curves will differ a little from those shown in Fig. 4. The straight lines drawn through the black circles in Fig. 3 correspond to the section $\varphi = 9°$ (or 171°). Thus, the nuclei responsible for the echo signal are located for crystal 1 in a layer closer to the domain than for crystal 2.

We can conclude on the basis of the presented analysis that at least in fields exceeding 0.5–10 kOe the echo signals are due to nuclei whose coordinates remain practically unchanged. These nuclei are located in a certain "near-domain" layer. The depth of this layer in crystals of different quality can be different. This

is the main reason why the spin-echo spectra differ from the results obtained by the continuous procedure. In the last case, as already noted, the coordinates of the nuclei corresponding to the condition $d\omega(\varphi)/d\varphi = 0$, which determines the position of the lines, shift towards the center of the wall. The shift of the points corresponding to this condition is shown in Fig. 4 by arrows. This shift corresponds to curves 2 of Fig. 1.

We present a few more arguments in favor of the assumption that a certain "near-domain" layer exists and determines the nuclear echo signals.

First, this is attested to by the invariance of the relaxation time in a field $H_x > 1$ kOe (Table II). If the coordinates of the nuclei were to vary strongly, as is the case in the continuous procedure, then a strong dependence of T_1 and T_2 on H_x would inevitably be observed.

Second, with the aid of this assumption it is possible to explain qualitatively some features of the shapes of the spectra. It can be seen from Fig. 4 that as the domain is approached the frequency branches at $H_x = 0$ (thicker curves), closer together and tend in the limit to the "domain" frequency ν_d. In the layer with $\varphi = 18°$, the frequency branches are more strongly "separated" than for the layer with $\varphi = 9°$. This difference in the distribution of the resonance frequencies is apparently the reason why two maxima are resolved for crystal 2 in the spectrum at $H_x = 0$, and for crystal 1 there is observed only one asymmetrical line with a more gentle decline on the low-frequency side.

At $H_x \neq 0$, the two frequency branches begin to intersect. With increasing H_x, an instant should set in when the "overturning" point of the curves of Fig. 4 reaches the layer in which are located the nuclei responsible for the echo signals. This instant corresponds to the start of the splitting of the frequencies of Fig. 3. For crystal 2 this takes place in a field somewhat exceeding 1 kOe, while for crystal 1 in a field $H_x \approx 0.6$ kOe, inasmuch as in the latter case the layer is closer to the domain. This field should correspond in both cases to the highest homogeneity of the distribution of the frequencies over the resonant nuclei and their largest spectral density. Indeed, in the indicated fields the line shape (Fig. 2) becomes narrower and more symmetrical, and the line intensity increases.

Naturally, the discussed simple scheme, based on consideration of a definite sort of a fixed section inside the wall, cannot explain all the singularities, without exception, in the spin-echo signal. For example, it is seen from Fig. 3, that the points corresponding to the low-frequency maximum near $H_x = 0$, located near 75.5 MHz, does not fall on the line corresponding to $\varphi = 18°$.

In addition, the relaxation times for the low-frequency maximum at $H_x = 0$ (Table II) is approximately half as short as for the high-frequency maximum. It follows therefore that the low-frequency echo signal in a zero field is produced by nuclei located somewhat deeper in the wall compared with the high-frequency signal. Their localization, however, still corresponds to smal-

ler angles φ than for the "stationary" line $\nu_{min} = 75.4$ MHz, which corresponds to an angle $\varphi = 58°$ (122°) (marked by the lowest arrow on Fig. 4). In addition, in weak fields $H_x < 0.5$ kOe, some changes occur inside the wall. They have not been taken into account by us, and are connected with the redistribution of the contributions of the different nuclei to the echo signals, which lead to a certain shortening of the relaxation time compared with the values at $H_x = 0$. In stronger fields, equalization of T_1 and T_2 takes place, and the results are adequately explained by assuming that the resonant nuclei are located in a non-variable "near-domain" wall near the wall.

The location of this layer inside the wall is determined apparently principally by a combination of relaxation characteristics and a gain that is "appropriate" for the experimental conditions. For nuclei near the center at T_{20}, indicated in Table II, the condition $T_2 < \tau_{12}$ will be satisfied. It is clear that in this case the echo will appear and it will be "forced" to be formed on nuclei located closer to the domain. However, observation of the echo from nuclei that are too close to the domain is hindered by the abrupt decrease of the gain as $\varphi \rightarrow 0$.

With the aid of (15) it is possible to estimate the values of T_2 for nuclei in layers with $\varphi = 18°$ (for crystal 2) and $\varphi = 9°$ (for crystal 1). The obtained values of T_2 (130 and 170 μsec) differ little from each other and are close enough to the experimental ones. This indicates, in particular, that the values of T_{20} chosen for the calculation are quite realistic. Since T_{20} for crystal 2 is five times larger than for crystal 1, the optimal value of T_2 for echo formation is reached at a larger depth than for crystal 1.

The causes of the shorter relaxation times at the center of the wall for a hydrothermal crystal can be similar to those which determine the difference between the values of the parameter α for the two compared crystals. These causes were discussed in §2.

CONCLUSION

The form of the spin-echo spectra for the ^{57}Fe nuclei in the domain walls of the $YFeO_3$ crystals and the character of the evolution of these spectra in an external field are determined to a great degree by the relaxation processes that take place inside the wall. The experimental spectra are satisfactory described by the spin-echo theory for domain walls only if account is taken of the changes of the relaxation time T_2 over the wall thickness and of the specifics of the distribution of the NMR frequencies inside the wall, due to the properties of the magnetic symmetry of the orthoferrites. Owing to the extremely short values of T_2 for the wall center, the echo signals were observed from nuclei located at the "edges" of the walls. In an external field, the echo continue to be formed in a definite "near-domain" layer, and this leads to an entirely different evolution of the spectra compared with the spectra obtained by the continuous procedure. The depth of this layer in the wall can vary from crystal to crystal. Its position is determined, in particular, by the shortest relaxation time T_{20} for the wall center, which in turn depends on the type and amount of impurities and on the perfection of the crystals. The form of the spin-echo crystals for crystals grown by different methods can therefore differ.

[1]A. V. Zalessky, A. K. Zvezdin, I. S. Zheludev, A. M. Savvinov, and A. F. Lebedev, Phys. Stat. sol. (b) 73, 317 (1976).

[2]A. V. Zalessky and I. S. Zheludev, Atomic Energy Review 14, 133 (1976).

[3]A. K. Zvezdin, Zh. Eksp. Teor. Fiz. 68, 1434 (1975) [Sov. Phys. JETP 41, 715 (1975)].

[4]S. Nadolski and W. Zbieranowski, J. Physique Suppl. 4, 38, CI-65 (1977).

[5]A. V. Zalesskiĭ and T. A. Khimich, Pis'ma Zh. Eksp. Teor. Fiz. 31, 194 (1980) [JETP Lett. 31, 178 (1980)].

[6]A. M. Balbashov and A. Y. Chervonenkis, Magnitnye materialy dlya mikroélektroniki (Magnetic Materials for Microelectronics), Énergiya, 1979.

[7]A. C. Goddard, A. M. Portis, M. Rubistein, and R. H. Lindquist, Phys. Rev. 128A, 1415 (1965).

[8]A. Hirai, J. A. Eaton, and C. W. Searle, Phys. Rev. 3B, 68 (1971).

[9]A. K. Zvezdin, Pis'ma Zh. Eksp. Teor. Fiz. 29, 605 (1979) [JETP Lett. 29, 553 (1979)].

[10]E. T. Jaynes, Phys. Rev. 98, 1099 (1955).

[11]A. L. Bloom, Phys. Rev. 98, 1105 (1955).

[12]M. B. Stearns, Phys. Rev. 162, 496 (1967).

Translated by J. G. Adashko